Journal of Structural Geology, Vol. 14, No. 2, pp. 237 to 244, 1992
Printed in Great Britain

0191-8141/92 $05.00+0.00

Critical stress difference, fault orientation and slip direction in anisotropic rocks under non-Andersonian stress systems

Z.-M. YIN and G. RANALLI*

Department of Earth Sciences and Ottawa-Carleton Geoscience Centre, Carleton University, Ottawa, Canada K1S 5B6

(*Received* 29 *November* 1990; *accepted in revised form* 25 *June* 1991)

Abstract—The Coulomb–Navier failure criterion is applied to geological faulting in the general three-dimensional case of rocks containing arbitrarily oriented strength anisotropies and subject to non-Andersonian stress systems (i.e. with none of the principal stresses acting in a vertical direction). General expressions for the critical stress difference necessary to cause failure as a function of depth are given in terms of material parameters, pore fluid pressure, orientation of the stress field and orientation of the strength anisotropy. The range of angles between a plane of anisotropy and the maximum principal stress direction, for which slip occurs along the pre-existing anisotropy rather than along a new fault, is calculated as a function of depth for different stress regimes.

When the stress field is non-Andersonian and/or strength anisotropies not containing the intermediate stress direction occur in the rock, faulting generally is oblique-slip. A kinematic classification of faulting is given on the basis of the angle between the strike direction and the slip direction on the fault plane. Triangular diagrams, analogous to those used in petrology, are introduced to describe (i) faulting in isotropic rock subject to arbitrarily oriented stress fields, and (ii) faulting in anisotropic rock when one principal stress direction is vertical. The type of faulting as a function of stress field and anisotropy orientation can be read off directly from these diagrams.

INTRODUCTION

SHEAR faulting in the upper lithosphere is usually described in terms of the Coulomb–Navier brittle failure criterion (see e.g. Jaeger & Cook 1969, Ranalli 1987, Mandl 1988). Assuming one principal stress direction to be vertical, Anderson (1905, 1951) used this criterion to account for the orientation of normal, strike-slip and thrust faults. Sibson (1974) derived expressions for the critical stress difference in the three standard faulting regimes on planes with negligible cohesion most favourably oriented for failure. Ranalli & Yin (1990) extended Sibson's analysis to rocks containing strength anisotropies (i.e. pre-existing planes of weakness), and derived expressions for the critical stress difference and orientation of faulting in the two-dimensional anisotropic case under Andersonian stress systems.

Often, however, none of the three principal stress directions is vertical, i.e. the stress state is *non-Andersonian* (see e.g. the analyses of stress distributions in crustal blocks by Hafner 1951, Sanford 1959, Yin 1989, and the general discussion by Mandl 1988). Consequently, the problem arises of determining, given the orientation of the stress field, the critical stress difference necessary for faulting in both isotropic and anisotropic rocks in the general case when the planes of weakness are not parallel to the direction of intermediate stress, and the range of orientations (with respect to the principal stress system) for which faulting occurs on strength anisotropies rather than on new fault planes. This problem is addressed in this paper. The aim is to provide a simple extension of the Coulomb–Navier criterion which may be useful in the analysis of fault reactivation and tectonic inversion. We do not address the inverse problem, that is, the determination of the tectonic stress tensor from fault orientation and slip data (see e.g. Sassi & Carey-Gailhardis 1987, Célérier 1988). An attempt is also made at classifying oblique-slip faulting in terms of the orientation of principal stresses, strength anisotropies and slip directions.

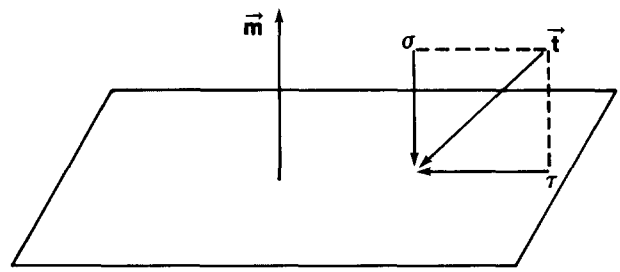

Fig. 1. Traction vector **t** with its normal (σ) and shear (τ) components on the horizontal plane of unit normal **m** with respect to the principal stress directions.

FORMATION OF NEW FAULTS IN ISOTROPIC ROCK

In a Cartesian co-ordinate system x_1, x_2, x_3 (corresponding to the direction of principal stresses $\sigma_1, \sigma_2, \sigma_3$, respectively), let **m** be the unit normal to the horizontal plane through the origin, where $m_i = \cos \alpha_i$ ($i = 1, 2, 3$), and α_i is the angle between the unit normal and the x_i-axis (Fig. 1). The traction vector **t** on the horizontal

*Also at: Institut für Mineralogie und Petrographie, ETH-Zentrum, CH-8092 Zürich, Switzerland.

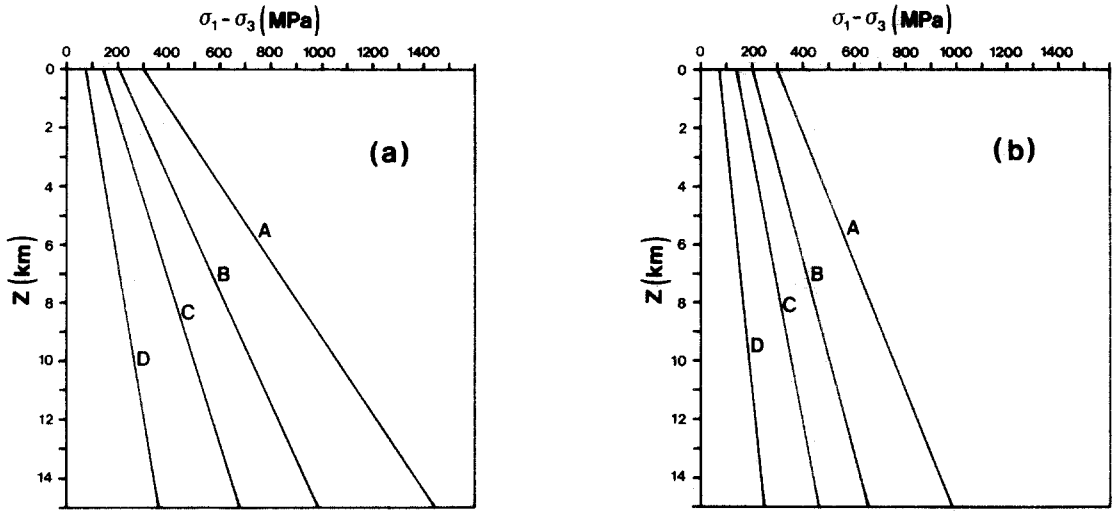

Fig. 2. Critical stress difference vs depth for faulting in isotropic rocks in the cases of (a) no pore fluid pressure ($\lambda = 0$) and (b) hydrostatic pore fluid pressure ($\lambda = 0.4$). Orientation of the stress field: (A) σ_3 vertical (thrust faulting); (B) $\alpha_1 = 80°$, $\alpha_2 = 60°$, $\alpha_3 = 32°$; (C) $\alpha_1 = 60°$, $\alpha_2 = 60°$, $\alpha_3 = 45°$; (D) σ_1 vertical (normal faulting). Parameters are $S = 75$ MPa, $\mu = 0.75$, $\rho = 2600$ kg m^{-3} and $\delta = \frac{1}{2}$.

plane has components (Jaeger & Cook 1969, p. 20, Mandl 1988, p. 204):

$$t_1 = -\sigma_1 m_1, \qquad t_2 = -\sigma_2 m_2, \qquad t_3 = -\sigma_3 m_3,$$

where signs have been chosen such that compressive stresses are positive, and the traction vector components are negative when pointing in the negative direction of the co-ordinate axes. The traction vector can be resolved into a normal and a shear component (σ and τ, respectively). The normal component is the overburden pressure

$$\sigma = \rho \mathbf{g} z(1 - \lambda), \tag{1}$$

where ρ is density, $\mathbf{g}$ acceleration of gravity, z depth, and λ the pore fluid factor (ratio of pore fluid pressure to overburden pressure). This component can also be obtained from

$$\sigma = \mathbf{t} \cdot (-\mathbf{m}) = \sigma_1 m_1^2 + \sigma_2 m_2^2 + \sigma_3 m_3^2 \tag{2}$$

which, putting $\sigma_2 = \sigma_3 + \delta(\sigma_1 - \sigma_3)$, $0 < \delta < 1$, and since $\mathbf{m}$ is a unit vector, becomes

$$\sigma = (m_1^2 + \delta m_2^2)(\sigma_1 - \sigma_3) + \sigma_3. \tag{3}$$

Comparing equations (1) and (3) one obtains for the maximum stress difference

$$\sigma_1 - \sigma_3 = \frac{\rho \mathbf{g} z(1 - \lambda) - \sigma_3}{m_1^2 + \delta m_2^2}. \tag{4}$$

The Coulomb–Navier failure criterion can be written as (Jaeger & Cook 1969, pp. 87–91)

$$\tfrac{1}{2}(\sigma_1 - \sigma_3) \sin 2\theta = S + \mu[\tfrac{1}{2}(\sigma_1 + \sigma_3) - \tfrac{1}{2}(\sigma_1 - \sigma_3) \cos 2\theta], \tag{5}$$

where S is cohesion, μ the coefficient of steady sliding friction, and θ the angle between the plane of failure (containing the σ_2-axis) and the σ_1 direction. Substituting equation (4) in (5), and using the relation $\theta = \frac{1}{2} \tan^{-1}(1/\mu)$, we obtain the following relation that holds at failure

$$\sigma_1 - \sigma_3 = \frac{2\mu\rho \mathbf{g} z(1 - \lambda) + 2S}{(\mu^2 + 1)^{1/2} - \mu + 2\mu(m_1^2 + \delta m_2^2)}. \tag{6}$$

Equation (6) gives the critical stress difference for Coulomb–Navier shear fracture in isotropic rock as a function of material parameters, depth and orientation of the principal stress field. The critical stress difference is shown in Fig. 2 as a function of depth for various orientations of the stress field and given values of material parameters.

In the particular case when one of the principal stress directions is vertical (Andersonian stress state), we obtain the following relations for the three classical faulting regimes.

Thrust ($\sigma_3 = \sigma, m_1 = m_2 = 0, m_3 = 1$):

$$\sigma_1 - \sigma_3 = \frac{2\mu\rho \mathbf{g} z(1 - \lambda) + 2S}{(\mu^2 + 1)^{1/2} - \mu}. \tag{7a}$$

Normal ($\sigma_1 = \sigma, m_1 = 1, m_2 = m_3 = 0$):

$$\sigma_1 - \sigma_3 = \frac{2\mu\rho \mathbf{g} z(1 - \lambda) + 2S}{(\mu^2 + 1)^{1/2} + \mu}. \tag{7b}$$

Strike-slip ($\sigma_2 = \sigma, m_1 = m_3 = 0, m_2 = 1$):

$$\sigma_1 - \sigma_3 = \frac{2\mu\rho \mathbf{g} z(1 - \lambda) + 2S}{(\mu^2 + 1)^{1/2} + \mu(2\delta - 1)}. \tag{7c}$$

These equations, by introducing the principal stress ratio $R = \sigma_1/\sigma_3$, reduce to those derived by Sibson (1974) in the particular case $S = 0$, and by Ranalli & Yin (1990) for the more general case in which $S \neq 0$.

In many two-dimensional analyses of faulting (Hafner 1951, Sanford 1959, Yin 1989), it is assumed that the σ_2-axis is horizontal, and the σ_1- and σ_3-axes vary with

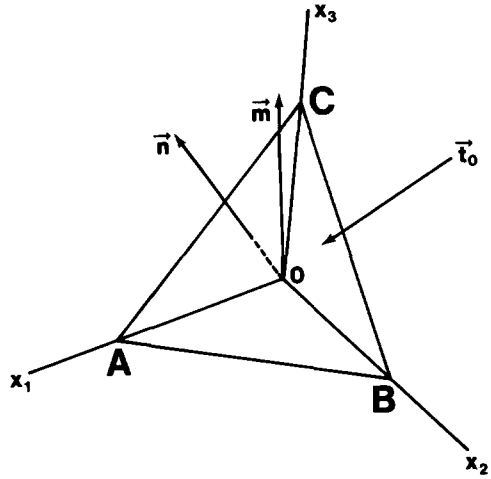

Fig. 3. Strength anisotropy (plane ABC with unit normal **n**) referred to principal stress system (x_1, x_2, x_3). The orientation of the unit normal vector to the horizontal plane and the traction vector acting on the anisotropy are denoted by **m** and $\mathbf{t}_0$, respectively.

position (this is the case, for instance, that leads to listric normal and thrust faults; see also Mandl 1988). For such a stress state ($m_2 = 0, m_1 \neq 0, m_3 \neq 0$) equation (6) reduces to

$$\sigma_1 - \sigma_3 = \frac{2\mu\rho\mathbf{g}z(1-\lambda) + 2S}{(\mu^2+1)^{1/2} + \mu(2m_1^2 - 1)}. \quad (8)$$

The critical stress difference required for failure depends on the orientation of the principal stress system, as the latter affects the normal stress on potential fracture planes. In order to predict occurrence and type of faulting, therefore, the determination of principal stress trajectories has to be followed by the determination of the stress difference as a function of position (see the discussion by Buck 1990 and Yin 1990).

SLIP ALONG PRE-EXISTING STRENGTH ANISOTROPIES

Now we assume that the rock contains planes of weakness of orientation defined by the unit normal **n** of components $n_i = \cos\gamma_i$, where γ_i is the angle between **n** and the x_i-axis (Fig. 3). The traction vector $\mathbf{t}_0$ acting on the plane of weakness has components $t_{01} = -\sigma_1 n_1$, $t_{02} = -\sigma_2 n_2$, $t_{03} = -\sigma_3 n_3$, and its magnitude is given by

$$t_0^2 = \sigma_1^2 n_1^2 + \sigma_2^2 n_2^2 + \sigma_3^2 n_3^2. \quad (9)$$

The traction vector can be resolved into a normal and shear component. The normal component, in a manner analogous to equation (3), can be written as

$$\sigma = (n_1^2 + \delta n_2^2)(\sigma_1 - \sigma_3) + \sigma_3. \quad (10)$$

The shear component can be obtained from the relation $\tau^2 = t_0^2 - \sigma^2$ which, after some algebra, yields

$$\tau = (\sigma_1 - \sigma_3)[(n_1^2 + \delta^2 n_2^2) - (n_1^2 + \delta n_2^2)^2]^{1/2}. \quad (11)$$

Thus the Coulomb–Navier criterion can be written as

$$(\sigma_1 - \sigma_3)[(n_1^2 + \delta^2 n_2^2) - (n_1^2 + \delta n_2^2)^2]^{1/2} = S_0 + \mu_0[(n_1^2 + \delta n_2^2)(\sigma_1 - \sigma_3) + \sigma_3], \quad (12)$$

where S_0, μ_0 are cohesion and coefficient of friction along the anisotropy. (In general, both S_0 and μ_0 will be less than the corresponding values in isotropic rock. Although we choose $\mu = \mu_0$ in the examples that follow, all relations are of general validity.) The minimum stress σ_3 can be expressed using equation (4) as

$$\sigma_3 = \rho\mathbf{g}z(1-\lambda) - (\sigma_1 - \sigma_3)(m_1^2 + \delta m_2^2). \quad (13)$$

Using equation (13) in (12) yields

$$\sigma_1 - \sigma_3 = \frac{\mu_0\rho\mathbf{g}z(1-\lambda) + S_0}{[(n_1^2+\delta^2 n_2^2) - (n_1^2+\delta n_2^2)^2]^{1/2} + \mu_0[(m_1^2+\delta m_2^2) - (n_1^2+\delta n_2^2)]}. \quad (14)$$

Equation (14), which reduces to the Andersonian case of Ranalli & Yin (1990) if the plane of weakness contains the σ_2-axis and one of the principal stress directions is vertical, gives the critical stress difference for faulting along a strength anisotropy as a function of depth, material parameters, and orientation of stress field and anisotropy. Examples are given in Fig. 4 for various orientations of the anisotropy and different material parameters.

At a given depth and for a given orientation of the stress field, faulting will occur along a plane of weakness only for a range of orientations, i.e. those for which the critical stress difference given by equation (14) is less than that given by equation (6). Outside this range, a new fault forms at an angle $\theta = \frac{1}{2}\tan^{-1}(1/\mu)$ with respect to the σ_1-axis and containing the σ_2-axis. By equating equations (14) and (6), the limiting angles can be expressed as

$$[n_1^2 + \delta^2 n_2^2 - (n_1^2 + \delta n_2^2)^2]^{1/2} - \mu_0(n_1^2 + \delta n_2^2) = \frac{\mu_0[(1+\mu^2)^{1/2} - \mu]}{2\mu} + \frac{\mu S_0 - \mu_0 S}{\mu(\sigma_1 - \sigma_3)}, \quad (15)$$

where the stress difference $(\sigma_1 - \sigma_3)$ is given by equation (6). For a given component n_i, equation (15) allows calculation of the ranges in the other two components consistent with faulting along pre-existing anisotropies. These reduce to the limiting angles given by Ranalli & Yin (1990) for anisotropies containing the σ_2-axis and vertical orientation of one of the principal stresses.

A graphic representation of the limiting angles is obtained by using the three-dimensional Mohr circle (see e.g. Jaeger & Cook 1969, pp. 27–29). With reference to Fig. 5, the three circles of radii $\frac{1}{2}(\sigma_2 - \sigma_3)$, $\frac{1}{2}(\sigma_1 - \sigma_3)$ and $\frac{1}{2}(\sigma_1 - \sigma_2)$ represent the stress states on planes with unit normal with components $n_1 = 0$, $n_2 = 0$ and $n_3 = 0$, respectively, the other two components being arbitrary in each case. Concentric circles (of which only two families are shown in the figure, for simplicity) represent stress states on planes on which a component $n_i = \cos\gamma_i$ is fixed. The two failure envelopes shown apply to intact rock (parameters S, μ) and strength anisotropies (S_0, μ_0). If for instance γ_2 is given, one can immediately read off the range in γ_1 for which a plane of

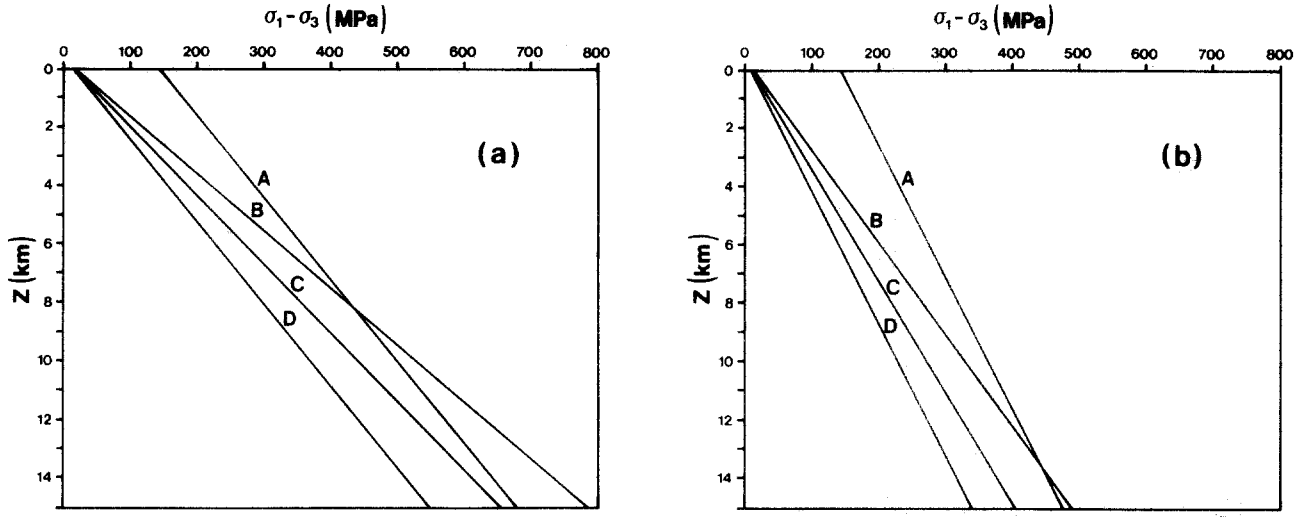

Fig. 4. Critical stress difference vs depth for faulting under a stress system of orientation $\alpha_1 = 60°$, $\alpha_2 = 60°$, $\alpha_3 = 45°$. (a) & (b) and isotropic parameters as in Fig. 2. Anisotropy parameters $S_0 = 5$ MPa, $\mu_0 = \mu$. (A) New fault in isotropic rock; (B) anisotropy with orientation $\gamma_1 = 55°$, $\gamma_2 = 60°$, $\gamma_3 = 50°$; (C) anisotropy with orientation $\gamma_1 = 70°$, $\gamma_2 = 60°$, $\gamma_3 = 37°$; (D) most favourably oriented strength anisotropy ($\gamma_1 = 90° - \frac{1}{2}\tan^{-1}(1/\mu_0)$, $\gamma_2 = 0$).

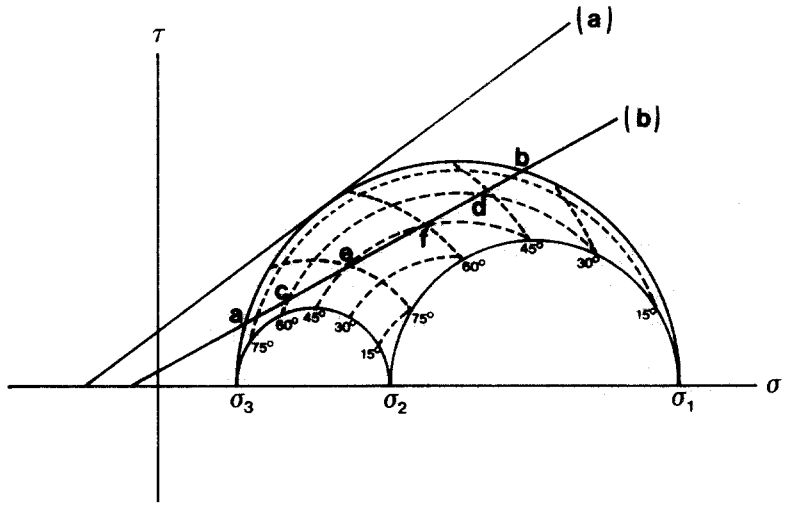

Fig. 5. Three-dimensional Mohr circle for failure in isotropic rock (envelope a) and along strength anisotropy (envelope b). Dashed circles concentric with full circle with diameter $\sigma_1 - \sigma_3$ represent stress states on planes with fixed γ_2; the other family represents stress states on planes with fixed γ_1. For a given γ_2, the range of γ_1 for which failure occurs along the anisotropy can be read from envelope (b). For instance, for $\gamma_2 = 90°$, the range of orientations is $a \geq \gamma_1 \geq b$; for $\gamma_2 = 60°$, $c \geq \gamma_1 \geq d$; and, for $\gamma_2 = 45°$, $e \geq \gamma_1 \geq f$.

weakness fails. The range in γ_3 can be calculated from the condition that **n** is a unit vector, or read off from a three-dimensional Mohr diagram on which all three families of circles are drawn. Figure 6 gives some examples of limiting angles for failure along strength anisotropies as a function of depth for various values of material parameters and orientation of the stress field. (Note that the limiting angle shown is the angle β between the plane of weakness and the σ_1-axis, while γ_1 above is the angle between the normal to the plane of weakness and the σ_1-axis.)

OBLIQUE-SLIP FAULTING

When the stress orientation is Andersonian and the fracture plane contains the intermediate stress direction, faulting is of necessity either purely dip-slip or purely strike-slip, and oblique-slip faulting (that is, with motion direction on the fault plane which forms an angle different from either 0° or 90° with the strike direction) does not occur. However, when restrictions on the orientation of both stress system and planes of weakness are dropped, oblique-slip faulting becomes possible. On the assumption that the direction of maximum shearing stress and the direction of slip on the fault plane coincide, we analyse in this section the general non-Andersonian case for anisotropic rocks (the Andersonian case has been considered by Bott 1959; see also Mandl 1988, pp. 203–206).

With reference to Fig. 7, let **h** be the unit strike vector in the horizontal direction on the fault plane referred to Cartesian co-ordinates coinciding with the principal stress directions. The maximum shear stress on the fault plane and its strike and dip components are denoted by τ, τ_h, and τ_d, respectively. The angle ω (measured in the

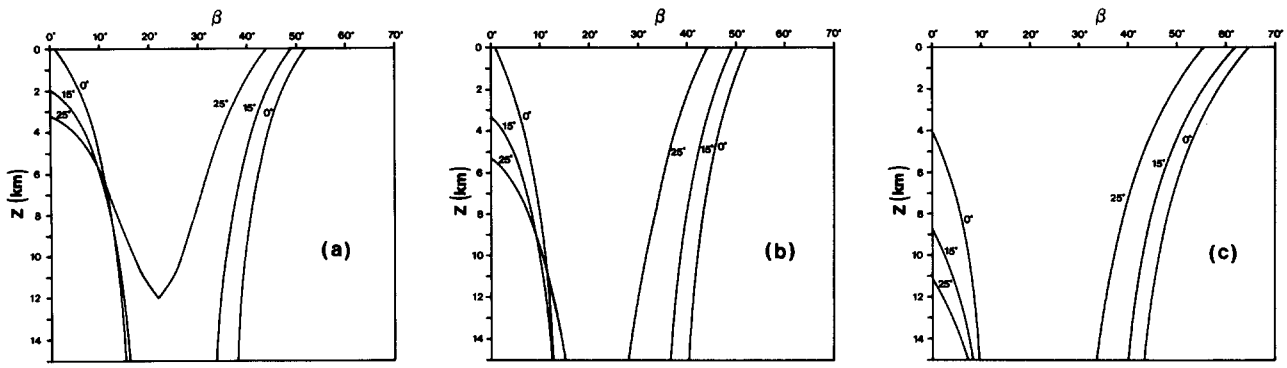

Fig. 6. Limiting angle β between strength anisotropies and maximum principal stress ($\beta = 90° - \gamma_1$) vs depth for slip along the anisotropy. Values on curves denote the angle between anisotropy and intermediate principal stress. (a) σ_3 vertical, $\lambda = 0$; (b) σ_3 vertical, $\lambda = 0.4$; (c) $\alpha_1 = 60°$, $\alpha_2 = 60°$, $\alpha_3 = 45°$, $\lambda = 0$. Parameters as in Fig. 4.

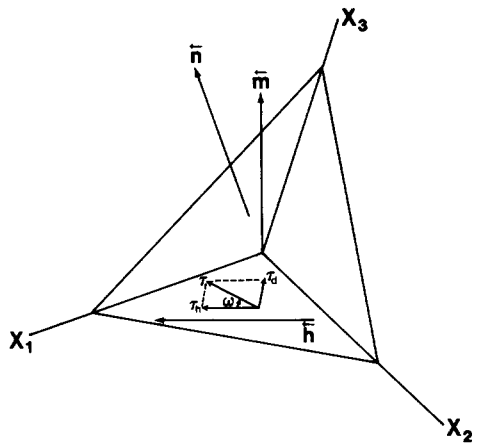

Fig. 7. Resolution of shear stress τ on fracture plane with normal **n** in the principal stress system with axes (x_1, x_2, x_3) with respect to the vertical **m**. The horizontal unit vector (along strike) is **h**. The strike and dip component of shear stress are τ_h and τ_d, respectively. The 'rake angle' ω gives the orientation of τ (and consequently of slip) with respect to the horizontal.

fault plane) giving the direction of τ, and therefore the slip direction, with respect to strike, is the quantity that we wish to express in terms of the orientation of the stress system (defined by the unit vector **m**) and the orientation of the fault plane (defined by the unit vector **n**). We call ω the 'rake angle' of slip. The signs of τ_h and τ_d are defined so that, if the unit vector **n** is upward, the leftward direction of τ_h and the upward direction of τ_d are positive (as in Fig. 7); if the vector **n** is downward, the leftward direction of τ_h and the downward direction of τ_d are positive. It follows that $0 \le n_i \le 1$ and $-1 \le m_i \le 1$ in each case.

Since the unit vector **h** is perpendicular to both **n** and **m** we can write

$$h_1 n_1 + h_2 n_2 + h_3 n_3 = 0$$
$$h_1 m_1 + h_2 m_2 + h_3 m_3 = 0$$
$$h_1^2 + h_2^2 + h_3^2 = 1$$

from which we obtain

$$h_1 = \frac{m_3 n_2 - m_2 n_3}{[(m_3 n_2 - m_2 n_3)^2 + (m_1 n_3 - m_3 n_1)^2 + (m_2 n_1 - m_1 n_2)^2]^{1/2}} \quad (16a)$$

$$h_2 = \frac{m_1 n_3 - m_3 n_1}{[(m_3 n_2 - m_2 n_3)^2 + (m_1 n_3 - m_3 n_1)^2 + (m_2 n_1 - m_1 n_2)^2]^{1/2}} \quad (16b)$$

$$h_3 = \frac{m_2 n_1 - m_1 n_2}{[(m_3 n_2 - m_2 n_3)^2 + (m_1 n_3 - m_3 n_1)^2 + (m_2 n_1 - m_1 n_2)^2]^{1/2}}. \quad (16c)$$

The strike component of the maximum shear stress is given by $\tau_h = \mathbf{t}_0 \cdot \mathbf{h}$, where $\mathbf{t}_0$ is the traction vector acting on the fracture plane; that is

$$\tau_h = -\sigma_1 n_1 h_1 - \sigma_2 n_2 h_2 - \sigma_3 n_3 h_3$$

and, using equations (16) and the identity $\sigma_2 = \sigma_3 + \delta(\sigma_1 - \sigma_3)$,

$$\tau_h = \frac{(\sigma_1 - \sigma_3)[(n_1 n_3 m_2 - n_1 n_2 m_3) - \delta(n_2 n_3 m_1 - n_1 n_2 m_3)]}{[(m_3 n_2 - m_2 n_3)^2 + (m_1 n_3 - m_3 n_1)^2 + (m_2 n_1 - m_1 n_2)^2]^{1/2}}. \quad (17)$$

The dip component is related to maximum shear stress and strike component by the relation $\tau_d^2 = \tau^2 - \tau_h^2$. Recalling equation (11) we can write

$$\tau_d = \pm(\sigma_1 - \sigma_3)\left\{(n_1^2 + \delta^2 n_2^2) - (n_1^2 + \delta n_2^2)^2 - \frac{[n_1 n_3 m_2 - n_1 n_2 m_3 - \delta(n_2 n_3 m_1 - n_1 n_2 m_3)]^2}{(m_3 n_2 - m_2 n_3)^2 + (m_1 n_3 - m_3 n_1)^2 + (m_2 n_1 - m_1 n_2)^2}\right\}^{1/2}. \quad (18)$$

Unlike equation (17), which gives both the magnitude and the sign of τ_h, equation (18) gives only the magnitude of τ_d. The sign of τ_d can be determined by the product of the cosine of the angle between τ and **m** and the cosine of the angle between **n** and **m**, i.e.

$$\cos(\tau, \mathbf{m}) \cos(\mathbf{n}, \mathbf{m}) = \frac{(n_1^2 + \delta n_2^2)(n_1 m_1 + n_2 m_2 + n_3 m_3)^2 - (n_1 m_1 + \delta n_2 m_2)(n_1 m_1 + n_2 m_2 + n_3 m_3)}{[(n_1^2 + \delta^2 n_2^2) - (n_1^2 + \delta n_2^2)^2]^{1/2}}. \quad (19)$$

If $\cos(\tau, \mathbf{m}) \cos(\mathbf{n}, \mathbf{m}) \le 0$, τ_d in equation (18) takes the plus sign; otherwise it takes the minus sign.

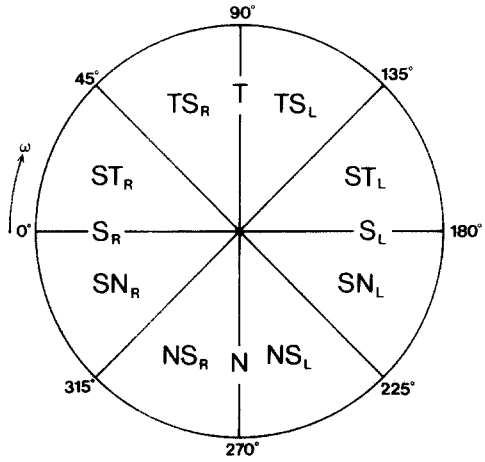

Fig. 8. Kinematic classification of faults based on the angle ω between the direction of slip and the horizontal. Purely normal, thrust and strike-slip faults are denoted by N, T and S, respectively. Combinations of letters denote oblique-slip faulting, with the first letter referring to the predominant component of slip. Subscripts L and R denote left-lateral and right-lateral slip, respectively.

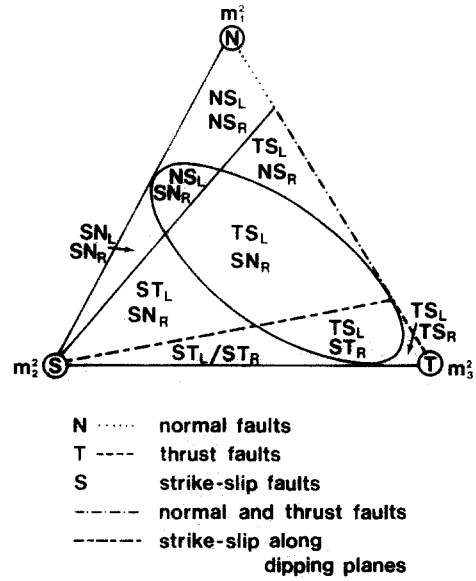

Fig. 9. Faulting regimes in isotropic rock as a function of the orientation **m** of the stress system. In each field within the triangle, two conjugate sets of faults are possible, as indicated. Normal, thrust and strike-slip faults of Andersonian type occur only at the vertices. For $m_2 = 0$ (horizontal intermediate stress direction) and mid-range values of m_1 and m_3, normal and thrust faults can coexist in conjugate sets. Strike-slip along dipping planes can occur for a fixed m_1/m_3 ratio.

The rake angle is therefore given by

$$\tan\omega = \frac{\tau_d}{\tau_h} = \pm\left\{\frac{[(n_1^2+\delta^2 n_2^2)-(n_1^2+\delta n_2^2)^2][(m_3n_2-m_2n_3)^2 + (m_1n_3-m_3n_1)^2+(m_2n_1-m_1n_2)^2]}{[n_1n_3m_2-n_1n_2m_3-\delta(n_2n_3m_1-n_1n_2m_3)]^2}-1\right\}^{1/2} \quad (20)$$

The value of the rake angle depends on the signs of τ_h and τ_d. For $\tau_h > 0$, $\tau_d \geq 0$, $0° \leq \omega < 90°$; for $\tau_h \leq 0$, $\tau_d > 0$, $90° \leq \omega < 180°$ for $\tau_h < 0$, $\tau_d \leq 0$, $180° \leq \omega < 270°$; and for $\tau_h \geq 0$, $\tau_d < 0$, $270° \leq \omega < 360°$.

Equations (17), (18) and (20) give the strike component, the dip component and the rake angle of the maximum shear stress (and consequently the motion direction) on the fault plane, for any orientation of stress system and fault plane. Pure dip-slip and pure strike-slip faulting are particular cases, depending for their occurrence on the vertical orientation of one principal stress and either the absence or a particular orientation (containing the σ_2-axis) of strength anisotropies. In all other cases, faulting is oblique-slip.

A kinematic classification of faults, based on the value of the angle ω, is shown in Fig. 8. A similar classification, for the special case of Andersonian stress systems, has been given by Bott (1959), based on the relative values of principal stresses.

EXAMPLES

In order to predict the possible types of faulting under given conditions, we consider different cases separately. For the *formation of new faults in non-Andersonian stress systems*, the fracture plane contains the intermediate stress direction ($n_2 = 0$), and $n_1^2 + n_3^2 = 1$. Under these conditions, equations (17), (18) and (20) reduce to

$$\tau_h = \frac{n_1n_3m_2(\sigma_1-\sigma_3)}{[(m_1n_3-m_3n_1)^2+m_2^2]^{1/2}} \quad (21a)$$

$$\tau_d = \pm\frac{(m_3n_1-m_1n_3)n_1n_3(\sigma_1-\sigma_3)}{[(m_1n_3-m_3n_1)^2+m_2^2]^{1/2}} \quad (21b)$$

$$\tan\omega = \pm\frac{m_3n_1-m_1n_3}{m_2}. \quad (21c)$$

By substituting the appropriate value for the critical stress difference (i.e. equation 6 for the most general case), the strike and dip components of the maximum shear stress on the fault plane can be expressed in terms of material parameters, depth and orientation of the stress system.

The type of faulting along new fracture planes as a function of the orientation of the stress system can be determined from equations (21a)–(21c). As $m_1^2 + m_2^2 + m_3^2 = 1$, it is convenient to display the results on a triangular diagram, similar to the construction used in petrology, where the co-ordinates m_i^2 of any point are given by the distance from the side opposite to the vertex, where $m_i^2 = 1$. Figure 9 shows the different types of faulting in terms of the orientation of the stress system. Each point in the diagram represents two potential conjugate fault planes, containing the intermediate stress axis and making an angle $\theta = \frac{1}{2}\tan^{-1}(1/\mu)$ with the maximum stress direction. Results are presented for the case where, on a stereographic projection, the principal stress axes, $\sigma_1, \sigma_2, \sigma_3$, are arranged in anticlockwise order; if they are arranged in clockwise order the type of faulting does not change, but the sense of slip is reversed. Naturally, oblique-slip faulting is the rule, unless one principal stress direction is vertical or the σ_2-axis is horizontal. Also, pure strike-slip along dipping planes is possible. In situations where the orientation of

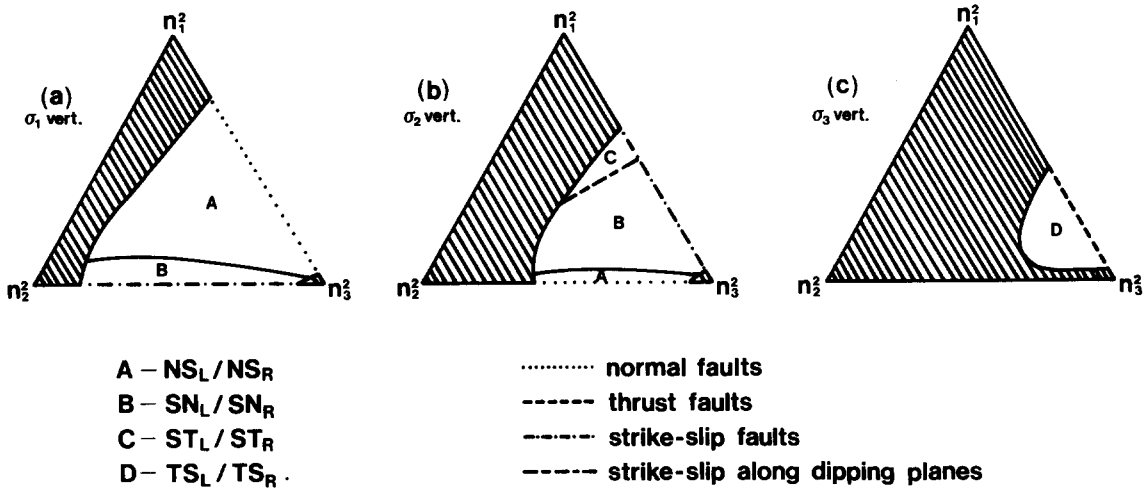

Fig. 10. Faulting regimes in rocks under Andersonian stress systems containing strength anisotropies as a function of the orientation **n** of the anisotropy. (a)–(c) refer to different vertical principal stress. Calculations are for $z = 10$ km, $S = 75$ MPa, $S_0 = 5$ MPa, $\mu = \mu_0 = 0.75$, $\rho = 2600$ kg m^{-3}, $\lambda = 0.4$ and $\delta = \frac{1}{2}$. The shaded areas denote values of **n** for which new faults (of the type appropriate to the vertical principal stress) form. Faulting along pre-existing planes of weakness, with slip as shown, occurs in the unshaded areas.

the stress system is known and the rock is isotropic, diagrams such as the one shown in Fig. 9, together with equations (21a)–(21c), allow the prediction of the fault plane orientation and slip direction.

Next we examine the case of an *Andersonian stress system in rocks containing strength anisotropies* (also considered by Mandl 1988, pp. 203–206). Under these conditions, new faults are pure dip-slip or strike-slip, but oblique-slip faulting can occur along anisotropies if they are favourably oriented. Three different faulting regimes are possible.

If σ_1 is vertical ($m_1 = \pm 1$, $m_2 = m_3 = 0$), equations (17), (18) and (20) become

$$\tau_h = \frac{-(\sigma_1 - \sigma_3)\delta n_2 n_3 m_1}{(n_2^2 + n_3^2)^{1/2}} \tag{22a}$$

$$\tau_d = \frac{\pm(\sigma_1 - \sigma_3)n_1[n_2^2(1-\delta) + n_3^2]}{(n_2^2 + n_3^2)^{1/2}} \tag{22b}$$

$$\tan\omega = \frac{\pm n_1[n_2^2(1-\delta) + n_3^2]}{\delta n_2 n_3}. \tag{22c}$$

If σ_2 is vertical ($m_1 = m_3 = 0$, $m_2 = \pm 1$), we have

$$\tau_h = \frac{(\sigma_1 - \sigma_3)n_1 n_3 m_2}{(n_1^2 + n_3^2)^{1/2}} \tag{23a}$$

$$\tau_d = \frac{\pm(\sigma_1 - \sigma_3)n_2[n_1^2(1-\delta) - \delta n_3^2]}{(n_1^2 + n_3^2)^{1/2}} \tag{23b}$$

$$\tan\omega = \frac{\pm n_2[n_1^2(1-\delta) - \delta n_3^2]}{n_1 n_3}. \tag{23c}$$

Finally, if σ_3 is vertical ($m_1 = m_2 = 0$, $m_3 = \pm 1$)

$$\tau_h = \frac{(\sigma_1 - \sigma_3)n_1 n_2 m_3(\delta - 1)}{(n_1^2 + n_2^2)^{1/2}} \tag{24a}$$

$$\tau_d = \frac{\pm(\sigma_1 - \sigma_3)n_3(n_1^2 + \delta n_2^2)}{(n_1^2 + n_2^2)^{1/2}} \tag{24b}$$

$$\tan\omega = \frac{\pm n_3(n_1^2 + \delta n_2^2)}{n_1 n_2(\delta - 1)}. \tag{24c}$$

The above relations reduce to those for normal, strike-slip and thrust faults, respectively, if faulting occurs along a new fracture plane ($n_2 = 0$). However, oblique-slip faulting takes place if favourably oriented planes of weakness are present. The results can be presented on triangular diagrams with co-ordinates n_i^2. Figure 10 illustrates both the limiting angles for faulting along strength anisotropies and the faulting regimes. (Note that the latter do not represent conjugate sets as in the isotropic case, but favourable orientations of strength anistropy along which a given type of slippage would occur.) The limiting angles are a function of depth (see equation 15); $z = 10$ km is the case shown. Faulting along strength anisotropies does not occur in the shaded areas where new faults form (normal, strike-slip or thrust according to which principal stress direction is vertical). Pure dip-slip and pure strike-slip faulting can occur along strength anisotropies which contain the σ_1- or σ_2-axis. In all other cases, faulting is oblique-slip. It can also be seen that a broad range of orientation is suitable for extensional reactivation, while a more restricted range is suitable for reactivation in compression.

Faulting in the most general case of non-Andersonian stress systems in rocks containing strength anisotropies can be predicted using the general equations (17), (18) and (20). However, the results cannot be simply presented on triangular diagrams.

CONCLUSIONS

The widespread occurrence of oblique-slip faults and of faults having dip angles other than those predicted for 'standard' stress states are indications of the existence of non-Andersonian stress systems and of fault reactivation. However, a general theory of faulting in anisotropic rocks under non-Andersonian stress systems has not been formulated so far. In this paper, we have provided simple expressions for the critical stress differ-

ence for Coulomb–Navier shear fracture in both isotropic rock and anisotropic rock as a function of material parameters, pore fluid pressure, depth, orientation of the stress field and orientation of anisotropies. These expressions can be used in stress analyses, to complement the calculation of stress magnitude and trajectories, in order to assess the likelihood of new faulting and fault reactivation in a given tectonic environment (see e.g. Yin 1989, and the discussion by Buck 1990 and Yin 1990).

An expression has also been given for calculating the limiting angles for failure for a strength anisotropy of arbitrary orientation as a function of material parameters, pore fluid pressure, depth and orientation of the stress field.This extends the previous two-dimensional treatment by Ranalli & Yin (1990), and makes it possible to extend to three dimensions two-dimensional analyses of fault reactivation and rotation (see e.g. Sibson 1985, Nur *et al.* 1986, 1989, Ivins *et al.* 1990). In this respect, it is interesting to note that the likelihood of reactivation varies in different tectonic regimes.

With respect to oblique-slip faulting, explicit expressions have been given for dip and strike components of the maximum shear stress and the slip direction on the fault plane, in terms of critical stress difference (that is, material parameters and depth) and orientations of stress system and strength anisotropy, thereby extending previous analyses by Bott (1959) and Mandl (1988).

These results have been synthesized graphically by means of triangular diagrams, where expected type of faulting is given as a function of stress orientation (for new fractures), or as a function of anisotropy orientation (for slip along pre-existing faults). A variety of tectonic environments, with their relevant faulting patterns, are thus amenable to analysis on the basis of a simple direct application of the Coulomb–Navier criterion.

Acknowledgements—This work has been made possible by an operating grant (to G. Ranalli) from the Natural Sciences and Engineering Research Council of Canada, with additional support from Carleton University and the Swiss Federal Institute of Technology (ETH). S. Thayer and L. Bender assisted with word-processing and drafting. We are grateful to Norman Fry and to an anonymous reviewer for suggestions to improve the paper.

REFERENCES

Anderson, E. M. 1905. The dynamics of faulting. *Trans. geol. Soc. Edin.* **8**, 393–402.

Anderson, E. M. 1951. *The Dynamics of Faulting and Dyke Formation* (2nd edn). Oliver & Boyd, Edinburgh.

Bott, M. H. P. 1959. The mechanics of oblique slip faulting. *Geol. Mag.* **96**, 109–117.

Buck, W. R. 1990. Comment on "Origin of regional, rooted low-angle normal faults: a mechanical model and its tectonic implications" by A. Yin. *Tectonics* **9**, 545–546.

Célérier, B. 1988. How much does slip on a reactivated fault plane constrain the stress tensor? *Tectonics* **7**, 1257–1278.

Hafner, W. 1951. Stress distribution and faulting. *Bull. geol. Soc. Am.* **62**, 373–398.

Ivins, E. R., Dixon, T. H. & Golombek, M. P. 1990. Extensional reactivation of an abandoned thrust: a bound on shallowing in the brittle regime. *J. Struct. Geol.* **12**, 303–314.

Jaeger, J. C. & Cook, N. G. W. 1969. *Fundamentals of Rock Mechanics* (3rd edn). Chapman & Hall, London.

Mandl, G. 1988. *Mechanics of Tectonic Faulting*. Elsevier, Amsterdam.

Nur, A., Ron, H. & Scotti, O. 1986. Fault mechanics and the kinematics of block rotations. *Geology* **14**, 746–749.

Nur, A., Ron, H. & Scotti, O. 1989. Kinematics and mechanics of tectonic block rotation. *Am. Geophys. Un. Geophys. Monogr.* **49**, 31–46.

Ranalli, G. 1987. *Rheology of the Earth*. Allen & Unwin, London.

Ranalli, G. & Yin, Z.-M. 1990. Critical stress difference and orientation of faults in rocks with strength anisotropies: the two-dimensional case. *J. Struct. Geol.* **12**, 1067–1071.

Sanford, A. R. 1959. Analytical and experimental study of simple geological structure. *Bull. geol. Soc. Am.* **70**, 19–51.

Sassi, W. & Carey-Gailhardis, E. 1987. Interprétation mécanique du glissement sur les failles: introduction d'un critère de frottement. *Annales Tectonicae* **1**, 139–154.

Sibson, R. H. 1974. Frictional constraints on thrust, wrench, and normal faults. *Nature* **249**, 542–544.

Sibson, R. H. 1985. A note on fault reactivation. *J. Struct. Geol.* **7**, 751–754.

Yin, A. 1989. Origin of regional, rooted low-angle normal faults: a mechanical model and its tectonic implications. *Tectonics* **8**, 469–482.

Yin, A. 1990. Reply. *Tectonics* **9**, 547–549.